Oncogene (2013) **32,** 2891–2899

www.nature.com/onc

ORIGINAL ARTICLE

Epigenetic-induced repression of microRNA-205 is associated with MED1 activation and a poorer prognosis in localized prostate cancer

T Hulf[1,7], T Sibbritt[1], ED Wiklund[1,2], K Patterson[1], JZ Song[1], C Stirzaker[1], W Qu[1], S Nair[1], LG Horvath[1,3], NJ Armstrong[1,4], JG Kench[1,5], RL Sutherland[1] and SJ Clark[1,6]

Deregulation of microRNA (miRNA) expression can have a critical role in carcinogenesis. Here we show in prostate cancer that miRNA-205 (miR-205) transcription is commonly repressed and the *MIR-205* locus is hypermethylated. *LOC642587*, the *MIR-205* host gene of unknown function, is also concordantly inactivated. We show that miR-205 targets mediator 1 (*MED1*, also called *TRAP220* and *PPARBP*) for transcriptional silencing in normal prostate cells, leading to reduction in *MED1* mRNA levels, and in total and active phospho-MED1 protein. Overexpression of miR-205 in prostate cancer cells negatively affects cell viability, consistent with a tumor suppressor function. We found that hypermethylation of the *MIR-205* locus was strongly related with a decrease in miR-205 expression and an increase in *MED1* expression in primary tumor samples ($n = 14$), when compared with matched normal prostate ($n = 7$). An expanded patient cohort (tumor $n = 149$, matched normal $n = 30$) also showed significant *MIR-205* DNA methylation in tumors compared with normal, and *MIR-205* hypermethylation is significantly associated with biochemical recurrence (hazard ratio = 2.005, 95% confidence interval (1.109, 3.625), $P = 0.02$), in patients with low preoperative prostate specific antigen. In summary, these results suggest that miR-205 is an epigenetically regulated tumor suppressor that targets *MED1* and may provide a potential biomarker in prostate cancer management.

Oncogene (2013) **32,** 2891–2899; doi:10.1038/onc.2012.300; published online 6 August 2012

Keywords: microRNA; miR-205; MED1; epigenetics; prostate cancer

INTRODUCTION

A prevailing concern in prostate cancer prognosis and treatment decisions is the absence of reliable markers for disease progression. In recent years, epigenetic modifications, such as DNA methylation and chromatin modification, have been shown to be sufficient to drive cancer phenotypes[1] and be of prognostic value.[2] MiRNAs (microRNAs) are noncoding RNAs that regulate gene expression in many biological processes including growth, differentiation, metabolism and development. MiRNAs typically exert a physiological effect through targeting mRNAs for repression. The paradigm for miRNA function at an mRNA target describes the degree of Watson–Crick base pairing between the miRNA seed sequence 2–8 and the target mRNA 3′-UTR determining the method of repression; with perfect complimentarity permitting Argonaut catalyzed degradation, and imperfect pairing promoting repression of translation.[3]

Recent studies have indicated that miRNAs are mechanistically involved in many human cancers,[4] including prostate cancer.[5] Moreover, miRNA expression profiles have proved to be superior to mRNA profiling for tissue and disease categorization.[6] However, a great many challenges remain in deciphering the regulation and role of miRNAs in normal and neoplastic tissue. MiR-205 exemplifies the challenge of understanding the role of miRNAs in cancer, in that studies on a range of cancers and cell lines have shown both positive and negative correlations between miR-205 expression and disease state. We recently identified both primary and mature miR-205 expression to be downregulated in prostate cancer cells.[7] MiR-205 expression has also been reported to be downregulated in a number of other cancers and cancer cell-line studies including: breast,[8–10] prostate,[11] bladder,[12] head and neck squamous cell carcinoma[13] and esophageal.[14] Conversely, miR-205 has been reported to be overexpressed in endometrial carcinoma,[15] ovarian,[16] non-small-cell lung cancer,[17–19] head and neck squamous cell carcinoma,[20–22] bladder,[23,24] and esophageal squamous mucosa.[25] A number of explanations may account for this, including the difficultly in controlling for normal tissue contaminating tumor samples. However, it is plausible that miR-205 expression levels are intrinsically linked with tumor progression and that different published expression changes may reflect tumor staging of individual cohorts. This possibility is supported by the fact that miR-205 is typically robustly expressed in epidermal tissues,[24] and is downregulated during epithelial to mesenchymal transition,[26] a mechanism whereby cells undergo loss of cell adhesion and increased cell mobility in a manner similar to the initiation of metastasis. Individual miRNAs may target numerous mRNA targets.[27,28] MiR-205 has previously been cited as targeting *HER3* (*ERBB3*),[9] *PKCe*,[11] *SHIP2* (*INPPL1*),[21] *VEGF-A*,[8] *SIP1* and *ZEB1*[26] for repression. In addition, miR-205 has been

[1]Epigenetics Group, Cancer Research Program, Garvan Institute of Medical Research, Darlinghurst, New South Wales, Australia; [2]Department of Molecular Biology, Aarhus University, Aarhus, Denmark; [3]Department of Medical Oncology, Sydney Cancer Center, Royal Prince Alfred Hospital, Camperdown, New South Wales, Australia; [4]School of Mathematics and Statistics, University of New South Wales, Sydney, New South Wales, Australia; [5]Department of Tissue Pathology, Royal Prince Alfred Hospital, Camperdown, New South Wales, Australia and [6]St Vincent's Clinical School, University of NSW, St Vincent's Hospital, Darlinghurst, New South Wales, Australia. Correspondence: Professor SJ Clark, Epigenetics Group, Cancer Research Program, Garvan Institute of Medical Research, 384 Victoria Street, Darlinghurst, New South Wales 2010, Australia.
E-mail: s.clark@garvan.org.au
[7]Current address: Sydney Medical School, Edward Ford Building (A27), Fisher Road, The University of Sydney, New South Wales 2006, Australia.
Received 2 November 2011; revised 15 May 2012; accepted 27 May 2012; published online 6 August 2012

shown to activate *IL24* and *IL32* by targeting sites in their promoters.[29] Recently, miR-205 was demonstrated to target mediator complex subunit 1 (mediator 1 (*MED1)*; also known as *PPARBP*, *CRSP1*, *PBP*, *RB18A* and *TRAP220*) in primary human trophoblasts.[30] *MED1* associates with the mediator complex, which functions as a molecular bridge between enhancer-bound activators, such as androgen receptor (AR), and the basal transcription machinery,[31] and is indispensable for transcription of selected AR targets.[32]

Here, we show that miR-205 is epigenetically silenced in prostate cancer, and is associated with DNA hypermethylation, H3K9-deacetylation and reduced mature miRNA expression in prostate cancer cells. Further, we demonstrate miR-205′s ability to inhibit proliferation in LNCaP cells, in a manner consistent with a role as a tumor suppressor. We find that *MED1*, which is overexpressed in prostate cancer cells, is knocked down or further upregulated by transient addition of miR-205 precursors or inhibitors, respectively. We show that in human prostate adenocarcinomas the miR-205 genomic locus is DNA hypermethylated, shows a reduction in miR-205 expression and has increased *MED1* expression. Importantly, high *MIR-205* DNA methylation is associated with relapse in patients with low preoperative prostate specific antigen (PSA).

RESULTS

miR-205 is epigenetically repressed in prostate cancer cells

The *MIR-205* gene is located on chromosome 12 and lies intragenic at the 3′ end of the predicted protein-coding gene of *LOC642587* (Figure 1a). *MIR-205* spans the intron–exon boundary of *LOC642587* (Figure 1a). To assess the expression and potential epigenetic regulation of miR-205 in prostate cancer, we cultured LNCaP metastatic prostate cells and prostate epithelial cells (PrEC) normal prostate epithelial cells both with and without the demethylating drug 5-Aza-2′-deoxycytidine (5-Aza-CdR, Fluka, St Louis, MO, USA). We used the miR-205 TaqMan quantitative PCR assay to quantify mature miR-205 expression, which revealed low expression of miR-205 in LNCaP cells relative to PrEC and a 40-fold increase in LNCaP cells in response to 5-Aza-CdR treatment ($n=3$, $P<0.001$; Figure 1b). Reexpression of miR-205 in response to 5-Aza-CdR, suggests epigenetic repression of this locus in the LNCaP cells. Therefore, we investigated the extent of both the repressive epigenetic marker, DNA methylation, and the active chromatin marker, H3K9 acetylation (H3K9Ac), at the *MIR-205* locus.

The *MIR-205* promoter has not been described and the genomic region surrounding *MIR-205* is relatively deplete in linear sequences of cytosine and guanine nucleotides (CpG sites). It contains no defined CpG island. We therefore designed a Sequenom MassArray (Sequenom, San Diego, CA, USA). MALDI-TOF mass-spectrometry assay to quantitate DNA methylation across the *MIR-205* genomic locus. This revealed strong and consistent enrichment of DNA methylation in LNCaP cells compared with PrEC cells across the five CpG MassArray units, representing seven CpG sites in total (Figure 2a, Supplementary Figure S2). To explore the DNA methylation pattern in more detail we designed bisulphite clonal sequencing assays to span both the *MIR-205* gene (Figure 1a). In agreement with the MassArray data, we found extensive DNA methylation in LNCaP cells and almost complete absence of DNA methylation in PrEC at the *MIR-205* locus (Figure 2b). To investigate if *LOC642587* expression is also under epigenetic control we used quantitative reverse transcription–PCR (qRT–PCR) to show that *LOC642587* is robustly expressed in PrEC and undetectable in LNCaP. In contrast to miR-205, however, treatment with 5-Aza-CdR did not induce *LOC642587* expression (Figure 1c) despite showing significant methylation in LNCaP cells (Figure 2c). Further to this we found treatment with histone deacetylase inhibitor trichostatin A, alone and in combination with 5-Aza-CdR, did not induce expression of LOC642587 in LNCaP cells (data not shown), suggesting repression of this transcript is more complex than DNA methylation and histone deacetylation.

Acetylation of histone H3 at lysine 9 (H3K9Ac) is one of the most commonly described epigenetic marks and is typically enriched in the promoter region of actively transcribed genes in euchromatic regions.[33] To determine H3K9Ac occupancy we performed chromatin immunoprecipitation (ChIP) followed by qPCR quantification at two loci (ChIP1/ChIP2), upstream and spanning the *MIR-205* locus (Figure 1a). Both loci showed depletion of H3K9Ac in LNCaP cells, but enrichment in PrEC cells (Figure 2d). Thus, the epigenetic status of the *MIR-205* locus reliably reflects the associated gene expression and suggests that epigenetic modification of the locus has an important role in silencing of miR-205 expression in the prostate cancer cells.

To investigate the prevalence of the epigenetic state and expression of miR-205 in other cancer cell lines we measured mature miRNA expression and DNA methylation of *MIR-205* in two additional metastatic prostate cancer cell lines, DU145 and PC3 and two metastatic breast cancer cell lines, MCF7 and MB231. Figure 2d displays the average relative DNA methylation determined by the MassArray assay at the *MIR-205* genomic locus, and shows that DU145 and PC3 are also DNA hypermethylated. Furthermore, mature miR-205 expression strongly inversely correlated with DNA methylation (Figure 2f), whereas low DNA methylation correlated with high expression of the mature miRNA in the normal cell line, PrEC. Similarly, higher expression correlated with low methylation in the normal breast cell lines HMEC184 and HMEC219, and lower expression correlated with higher methylation in the metastatic breast cancer cell lines MCF7 and MB231 (Figures 2e and f).

miR-205 functions as an inhibitor of cell viability

The cancer-associated changes in miR-205 expression shown in this and previous studies suggest that miR-205 has a role in cancer development. We investigated whether this is due to a primary silencing of miR-205 or a consequence of deregulation of the host gene *LOC642587*. In order to characterize the role of miR-205 alone in the control of prostate cell viability, we examined the effect of transient miR-205 overexpression in LNCaP cells using synthetic miRNA precursor molecules (pre-miR, Invitrogen, Carlsbad, CA, USA). Given the important role androgen signaling has in advanced prostate cancer,[34] we explored the impact of miR-205 overexpression both in the presence and absence of the androgen dihydrotestosterone (DHT). LNCaP cells were transfected in serum-free medium for 12 h, before the addition of fresh media with or without DHT. Seventy-two hours after transfection, cell viability was determined using the MTS assay. Cell viability was significantly reduced in pre-miR-205 transfected cells treated with DHT when compared with untransfected or pre-miR-scramble control ($P<0.03$), but was not significantly changed in the absence of DHT (Figure 3a). Our results show that miR-205 can negatively affect cell viability in prostate cancer cells, an effect consistent with tumor suppressor activity. In the light of these data we decided to concentrate our investigation on miR-205 and to identify a mechanism by which it might exert a tumor-suppressive effect.

miR-205 targets MED1

MED1 was recently shown to be a target of miR-205 in primary human trophoblasts.[30] Independently, we used three target prediction databases; pictar4way, Targetscan and miRanda, and found *MED1* to be one of 24 targets consistently predicted for miR-205 (Supplementary Figure S1A). Performing the reverse bioinformatic query returned only one consistent miRNA predicted to target the *MED1* 3′-UTR: miR-205 (Supplementary Figure S1B). The *MED1* 3′-UTR contains four miR-205 target seed sites, three of which are highly conserved (Supplementary Figure S1C).

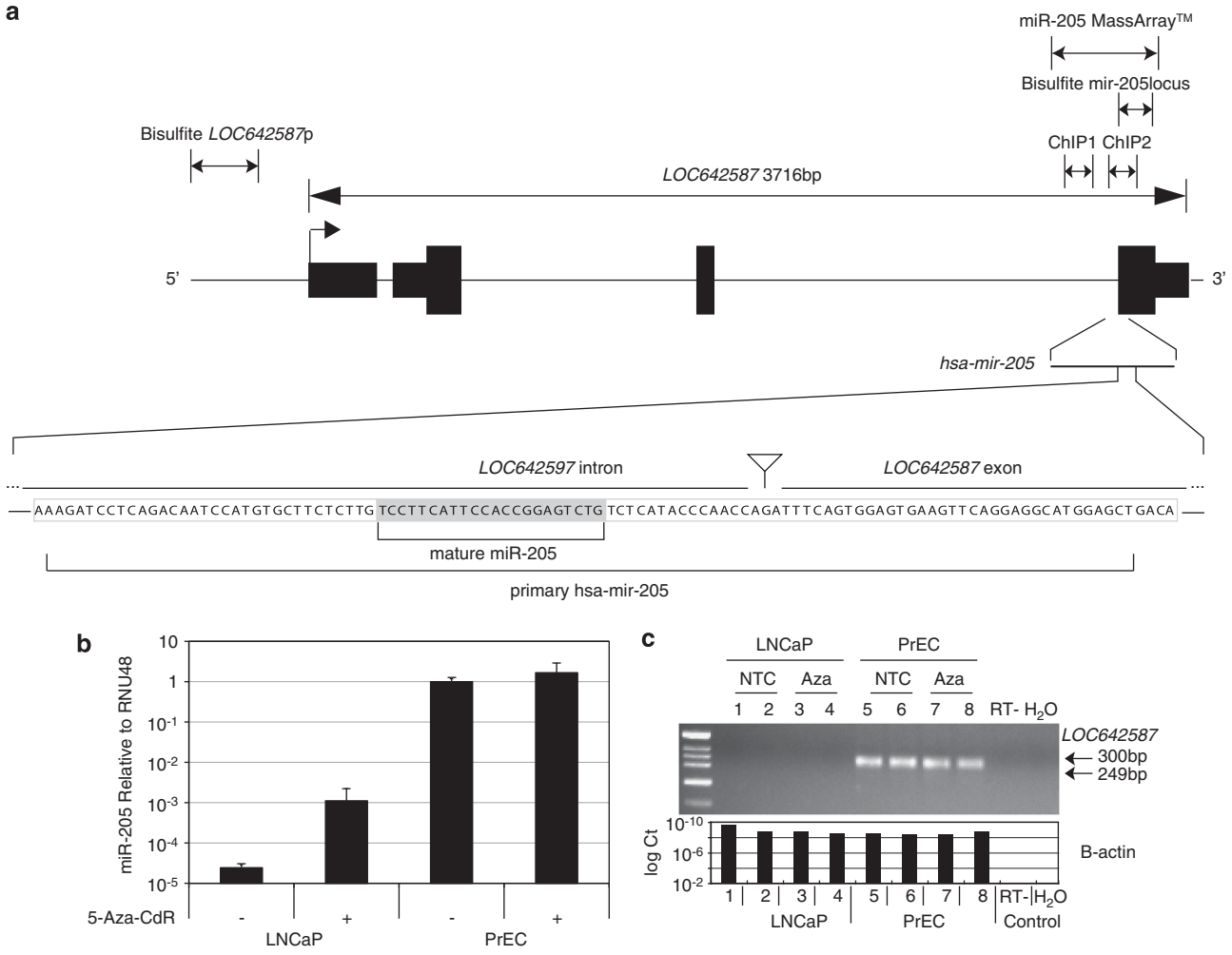

Figure 1. MiR-205 and *LOC642587* have reduced expression in prostate cancer cell line LNCaP. (**a**) Schematic of the *MIR-205* genomic location within the predicted gene *LOC642587* (Ref Seq Accession NM_001104548), and primer locations of DNA methylation (Bisulphite and MassArray) and ChIP assays (ChIP1/ChIP2) used in this study. (**b**) Quantitative RT–PCR of mature miR-205 expression normalized to RNU48, in LNCaP and PrEC cells with or without treatment with 5-Aza-CdR (**c**) *LOC642587* end point RT–PCR and β-*actin* TaqMan qRT–PCR performed in duplicate on LNCaP and PrEC cells that were either treated with 5-Aza-CdR (Aza, lanes 3, 4, 7 and 8) or untreated (non-transfected control (NTC), lanes 1, 2, 5 and 6). *LOC642587* PCR visualized by gel-electrophoresis migrating at approximately 300bp. Error bars represent standard error (s.e.).

Interestingly, *MED1* is a known AR coactivator and is critical for androgen dependent activation of AR target genes.[35] *MED1* is located at chromosome 17q12 and consists of 17 exons. To examine *MED1* expression we performed qRT–PCR spanning two different *MED1* introns (here named *med1_1* and *med1_2*; genomic locations are depicted in Supplementary Figure S1D), to account for possible expression disparity among splice variants. We found significantly increased expression of both *med1_1* and *med1_2* in LNCaP (for each assay, $P<0.01$; Figure 3b), supporting previously published results showing *MED1* overexpression in prostate cancer cell lines.[35] Treatment of these cell lines with 5-Aza-CdR caused a 10-fold reduction in expression of *med1_1* and *med1_2* in LNCaP cells ($P<0.01$), while expression remained relatively unchanged in PrEC (Figure 3b), consistent with the inductive effect of 5-Aza-CdR on miR-205 expression and subsequent downregulation of its target, *MED1*.

Next, to establish an explicit link between miR-205 expression and *MED1* repression, we performed qRT–PCR on both LNCaP and PrEC cells transfected either with pre-miR-205 or its respective scrambled control or with a miR-205 inhibitor, antisense locked nucleic acid (LNA, Exiqon, Vedbaek, Denmark), which is complementary to miR-205 or its respective scramble control. LNCaP cells transfected with pre-miR-205 exhibited a 30-fold downregulation of both *med1_1 and med1_2* amplicons when compared with the scramble control, while PrEC showed a twofold downregulation (for each amplicon, $P<0.05$; Figure 3c). As expected, treatment with LNA had the opposite effect, with a 16-fold increase in both *med1_1 and med1_2* compared with scramble control in LNCaP cells (for each amplicon, $P<0.05$; Figure 3c). However, there was no significant change in *MED1* expression in PrEC cells treated with the LNA-miR-205 inhibitor, possibly due to robust expression of miR-205 in PrEC limiting the efficacy of the inhibitor.

Total and phosphorylated-MED1 levels decrease in pre-miR-205 transfected cells

MED1 protein is phosphorylated by the mitogen-activated protein kinase extracellular signal-regulated kinase, whereupon it can associate with mediator complex.[36] We therefore examined both total and phosphorylated-MED1 levels in LNCaP and PrEC cells with or without transfection with pre-miR-205. Both the total and phosphorylated-MED1 protein expression were significantly higher in LNCaP than PrEC cells and importantly, transfection with pre-miR-205 led to a reduction in both total and phosphorylated-MED1 (Figure 3d). These results are consistent with *MED1* as a target of miR-205, and clearly demonstrate that

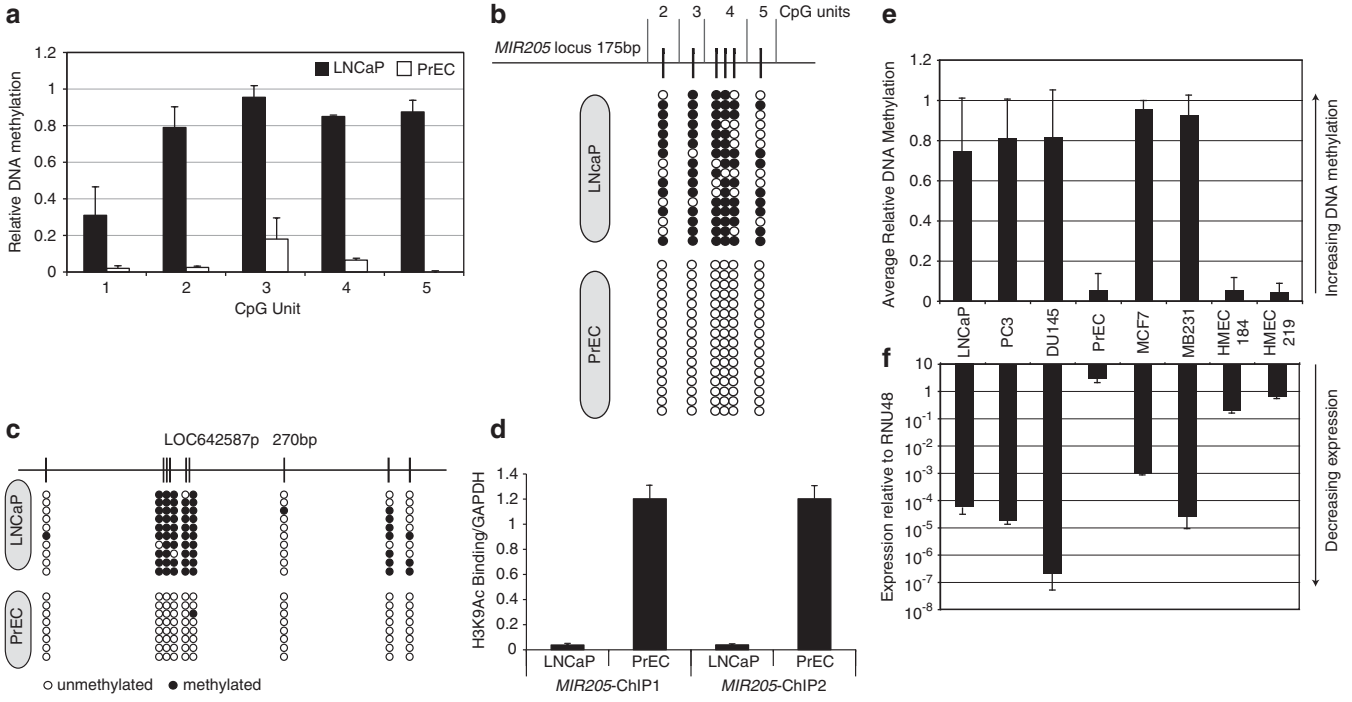

Figure 2. *Hsa-miR-205* is epigenetically silenced in prostate cancer cells. (**a**) DNA methylation of the *MIR-205* genomic region measured by MassArray mass-spectrometry five CpG units represent seven CpG sites, error bars represent s.e. (**b**) Bisulphite methylation clonal sequencing analysis at the *MIR-205* locus. White circles = unmethylated CpG sites; black circles = methylated CpG sites. (**c**) Bisulphite methylation clonal sequencing analysis at the *LOC642587p* locus. White circles = unmethylated CpG sites; black circles = methylated CpG sites. (**d**) H3K9Ac ChIP-PCR, at two loci proximal to miR-205, normalized to glyceraldehyde 3-phosphate dehydrogenase, error bars represent the s.e. (**e**, **f**) Three prostate cancer cell lines (LNCaP, PC3 and DU142) compared with normal prostate cell line PrEC, and two metastatic breast cancer cell lines (MCF7 and MB231) compared with two normal breast cell lines (HMEC184 and HMEC219) showing (**e**) *MIR-205* DNA methylation determined by MassArray mass-spectrometry and (**f**) MiR-205 mature transcript expression relative to RNU48. Error bars represent s.e.

increased expression of miR-205, whether by 5-Aza-CdR dependent endogenous activation or transfection of exogenous transcript, leads to *MED1* depletion.

MIR-205 is DNA hypermethylated in primary prostate adenocarcinomas

To investigate whether epigenetic miR-205 repression and targeting of *MED1* transcript occurred in primary prostate tumors, we performed DNA methylation and gene expression analyses in clinical prostate adenocarcinomas with matched normal samples where available. *MIR-205* DNA hypermethylation was evident in 14/14 tumors (Figure 4a) and the majority of the matched normal samples showed reduced DNA methylation, as determined by MassArray ($P = 0.03$, one-sided paired Wilcoxon). The 'long' MassArray assay was used for this experiment, schematically depicted in Supplementary Figure S2. DNA hypermethylation was confirmed in selected patient samples by clonal bisulphite sequencing (Figure 4b). The presence of some fully DNA methylated clones in the normal samples could reflect either a field effect or the presence of a small numbers of contaminating tumor cells.

Next, qRT–PCR was used to determine the expression of miR-205 in the tumor samples ($n = 7$). Consistent with the DNA methylation data, there was a trend towards increased expression of miR-205 in the normal samples compared with their respective matched tumors, with reduced but variable expression detected in the tumors overall (Figure 4c). Moreover expression of *MED1* was consistently lower in the matched normal tissue when compared with the tumor sections (Figure 4d, $P = 0.06$ 1-sided paired Wilcoxon). Together these results suggest that *miR-205* is DNA hypermethylated and repressed in prostate cancer, and may be associated with regulation of *MED1* levels *in vivo*.

MIR-205 DNA hypermethylation is related to a shorter time to biochemical relapse

MIR-205 DNA methylation was then assessed by Sequenom MassArray in a cohort of 149 patients treated with radical prostatectomy for localized prostate cancer, cohort described in Tables 1 and 2. Matched normal tissue was available for 30 of these samples. Pathological assessment of the radical prostatectomy specimens revealed 56.3% (84/149) of patients had organ-confined tumors, none had seminal vesicle involvement, <1% (1/149) had pelvic lymph node metastases and 40.3% (60/149) had surgical margins involved with tumor. The median trans-rectal biopsy Gleason score was 7 (range 5–9) and the median preoperative PSA was 7.6 ng/ml (range 1–50 ng/ml). At a median follow-up of 115 months (range 28–167 months), 45/149 (30.2%) had relapsed. Only three patients (2%) died of prostate cancer during the study period. Average *MIR-205* DNA methylation across the non-matched tumor samples ($n = 119$) showed significant increase compared with normal tissue ($P < 0.0001$, unpaired two-sided Wilcoxon, Figure 4e). Direct comparison of tumor and matched patient material ($n = 30$) showed an increase in tumor *MIR-205* DNA methylation in all but two samples (28/30, $P < 0.001$, paired two-sided Wilcoxon, Figure 4f).

We next looked for association with biochemical recurrence and *MIR-205* DNA methylation status. First, methylation status of the tumor samples was categorized into high and low based on the upper quartile of the median methylation values across the four CpG units depicted in the short MassArray schematic in Supplementary Figure S2. From this, we determined that high *MIR-205* DNA methylation was associated with a higher risk of biochemical relapse ($P = 0.002$, Figure 5). Furthermore, on multivariate analysis, low *MIR-205* methylation was a significant predictor of biochemical relapse ($P < 0.05$, Supplementary Table S1).

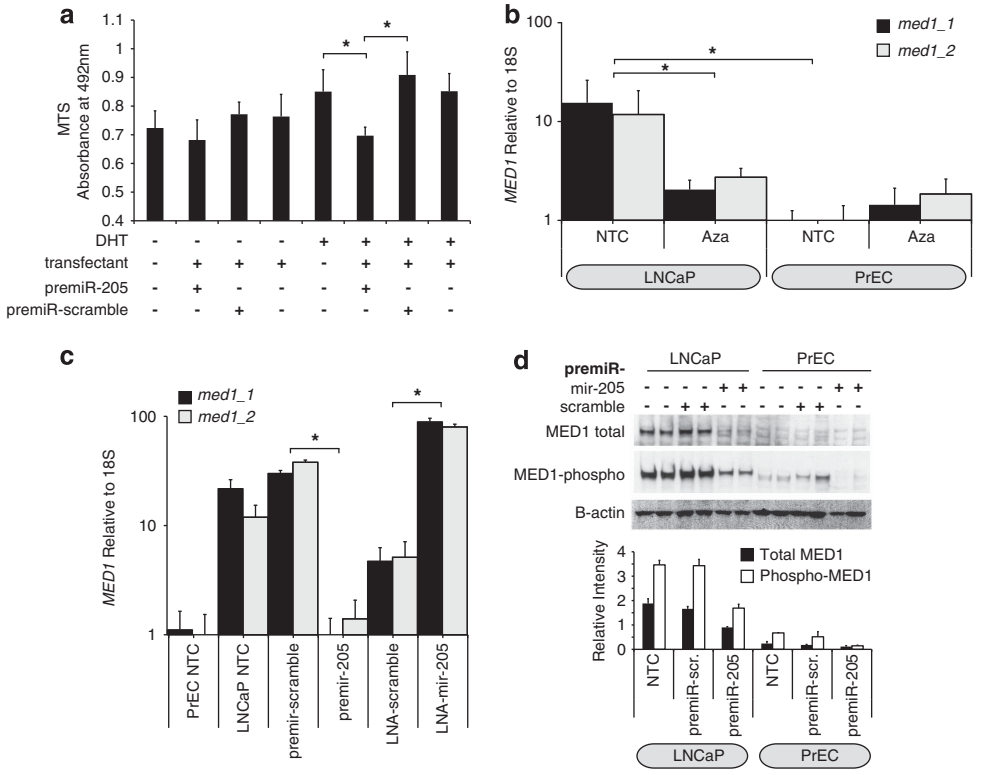

Figure 3. miR-205 inhibits cell viability and targets *MED1* in prostate cancer cells. (**a**) MTS assay showing absorption at 492 nm in LNCaP cells reverse transfected with either 50 nM pre-miR-205, scramble pre-miR control, or untreated, followed by incubation in media with or without DHT for 72 h. (**b**, **c**) Quantitative RT–PCR for *MED1* showing gene expression normalized to *18S*, and made relative to PrEC non-transfected control, error bars represent s.e. The two independent assays, *med1_1*, (black columns) and *med1_2* (gray columns) span introns at the 5′ and 3′ ends of *MED1,* respectively (see Supplementary Figure S1D for locations). (**b**) qRT–PCR *MED1* expression in LNCaP and PrEC cells with or without treatment with 5-Aza-CdR. (**c**) qPCR MED1 expression in PrEC or LNCaP cells reverse transfected with either 50 nM pre-miR-205, LNA-miR-205 inhibitor, respective scramble controls or untreated (NTC). (**d**) MED1 protein expression in LNCaP and PrEC cells determined by western blotting using antibodies against MED1, phosphorylated MED1 or β-actin as indicated. Densitometry shows normalized total MED1 (black columns) and phosphorylated MED1 (white columns), error bars represent s.e.

DISCUSSION

We recently showed that miR-205 DNA hypermethylation is both a hallmark of invasive bladder tumors and undifferentiated bladder cell lines,[37] and was identified in a high-throughput screen of epigenetic marks in prostate cancer cells.[7] Epigenetic mechanisms involved in miR-205 regulation in prostate cancer was also highlighted by Ke *et al.*,[38] where analyses using ChIP on promoter microarrays found gain of repressive H3K27-trimethylation in PC3 metastatic prostate cancer cells, and active H3K4-trimethylation in EP156T primary prostate epithelial cells proximal to the *MIR-205* locus. Here, we show that DNA methylation and histone H3K9-deacetylation of the miR-205 locus is associated with miRNA silencing and deregulation of MED1 in prostate cancer. Furthermore, high *miR-205* methylation predicted for a poorer prognosis in localized prostate cancer.

The function of specific miRNAs is best understood through its target genes. MiR-205 has a large number of predicted targets, several of which have now been confirmed. Using an unbiased approach we found *MED1* to be a predicted target of miR-205 *in silico*. The presence of four miR-205 target sites (three of which are highly conserved) in the *MED1* 3′-UTR suggests that miR-205 is important for *MED1* regulation, and occupation of one or more of these sites may result in nuclease catalyzed cleavage of the mRNA, in a manner recently described by Karginov *et al.*[39] The miR-205 *MED1* target relationship was also recently validated in primary human trophoblasts by Mouillet *et al.*,[30] however, a link between miR-205 deregulation and *MED1* has not been demonstrated in cancer. MED1 is a component of the mediator complex—a multi-subunit coactivator complex whose composition is intrinsically important for action of the transcription machinery.[40] MED1 was originally identified as overexpressed in 50% of a cohort of primary breast cancers; however only 24% of these cases were associated with gene amplification at the *MED1* locus,[41] suggesting that in approximately half of the cases, MED1 overexpression occurred independent of chromosomal events. This could be due to stabilization of MED1 transcript or protein, or alternatively, through reduction of repressors that target *MED1*, such as miR-205.

In agreement with previous studies, we found that *MED1* is elevated in prostate cancer compared with normal prostate cells, and in 5/7 prostate tumors compared with normal. Further, we have demonstrated that *MED1* is downregulated by 5-Aza-CdR treatment, suggesting that *MED1* is a target of an miRNA repressed by DNA methylation, and consistent with the increase in miR-205 following treatment with 5-Aza-CdR. This effect was confirmed by the transfection of exogenous pre-miR-205 or competitive miR-205 inhibitors, which revealed repression and induction of *MED1,* respectively. The negative effect of miR-205 overexpression on cell growth is consistent with previous findings where knockdown of *MED1* by RNA-interference in LNCaP, PC3 and DU145 cells reduced cell proliferation.[35] MiR-205 has previously been found to induce apoptosis and cell cycle arrest and reduce the invasiveness of PC3 cells,[29] and consistent with its role in regulation of epithelial to mesenchymal transition,[26] induce epithelial like morphology on overexpression in DU145 and PC3 prostate cancer cells.[11] Our observation that the most significant

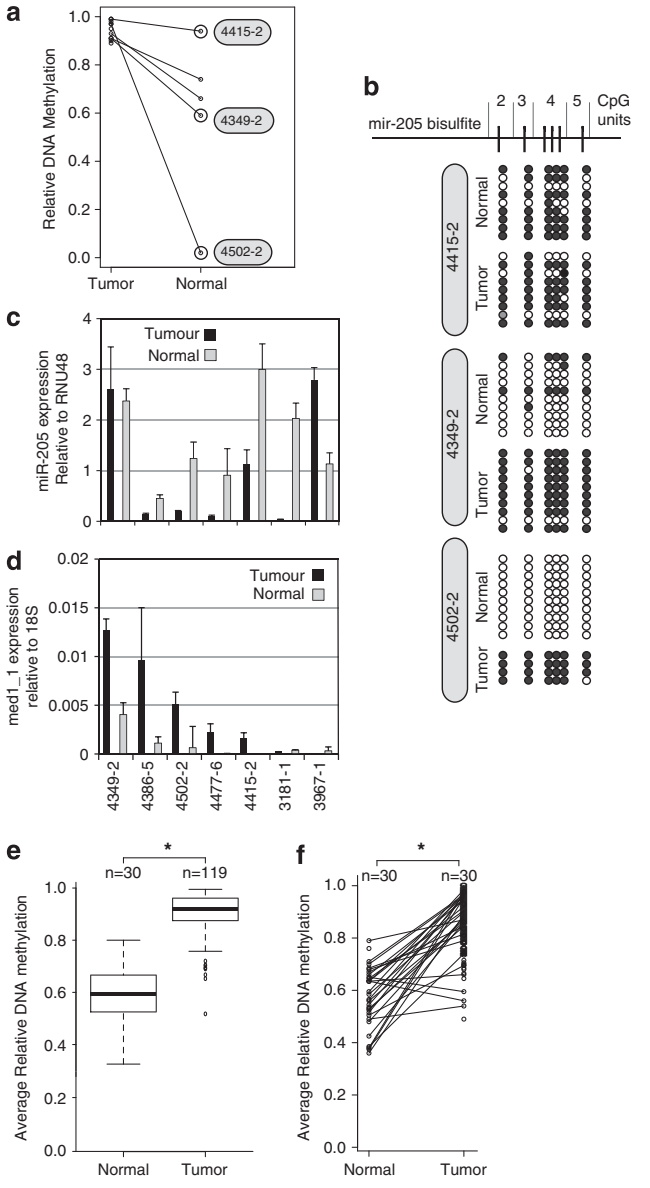

Figure 4. *MIR-205* DNA is hypermethylated and repressed in primary prostate cancer samples. (**a**) Strip chart showing average *MIR-205* DNA methylation (MassArray short: four CpG units, representing six CpGs; see Supplementary Figure S2) relative DNA methylation measured by MassArray mass-spectrometry. Lines connect patient tumor (total 14) with matched normal samples (five of the seven normal samples were successfully assayed). Labeled patient samples were chosen for clonal methylation analysis. (**b**) Bisulphite methylation clonal sequencing analysis at the *MIR-205* locus of three selected patients. White circles represent unmethylated CpG sites; black circles represent methylated CpG sites. (**c**) Mature miR-205 expression and (**d**) mRNA expression of *med1_1* in seven matched primary prostate samples determined by qRT–PCR, error bars represent s.d. (**e**) Box plot showing *MIR-205* DNA methylation in a larger cohort of prostate cancer samples (normal; $n = 30$, tumor; $n = 119$) (**f**) Strip chart showing *MIR-205* DNA methylation in individual patient matched tumor/normal samples ($n = 30$).

effect of miR-205 on cell growth in prostate cells is in the presence of androgen (DHT) is of particular interest. Androgen hormones regulate transcription of a number of genes through binding AR. Activated AR typically functions through migration to the nucleus and dimerization where it can bind to DNA, and through mechanisms that are yet to be fully described, can either activate or repress a variety of specific gene loci.[42] The mediator complex has been shown to be important for AR target activation,[32] and mediator complexes showing distinct subunit compositions have different transcriptional characteristics.[43] The mechanisms determining mediator complex composition and the principle components required for mediating transcription initiation at distinct sites remain unclear.[44] One potential instrument for varying mediator complex subunit composition, and thereby potentially altering the AR target gene profile, could be through miRNA directed transcriptional repression of mediator components. The androgen-specific growth effect of miR-205, shown here, could be reflective of this. A follow-up approach to this study would be to examine the growth effect of exogenous miR-205 in androgen-resistant prostate cancer cells, such as LNCaP-OM.[45] The effect of additional miRNAs that potentially target other mediator subunits on mediator composition and function would also be worthy of investigation. Given that the development of resistance to androgen depletion therapies is a determinative step in prostate cancer outcome, future studies will need to address the control of DNA methylation at *MIR-205* and the potential for this to modulate AR function, through dysregulation of *MED1* (Supplementary Figure S3).

We have previously shown an association between hypermethylation of coding genes within 2q14.2 and poor prognosis in prostate cancer.[46] Also, hypermethylation of *MIR124a* was recently shown to confer poor prognosis in acute lymphoblastic

Table 1. Overview of patient characteristics (continuous variables)

Variable	N	*Median*	*Minimum*	*Maximum*
Age at RP	149	61.0	47.6	74.30
Preoperative PSA (ng/ml)	149	7.6	1	50
Gleason score	148	7	5	9
Length of FUP (months)	149	115.3	27.5	167.4
Methylation level (average)	149	0.91	0.52	0.995

Abbreviations: FUP, follow up; PSA, prostate specific antigen; RP, radical prostatectomy. Note: tumor volume/percentage only available on <30 patients.

Table 2. Overview of patient characteristics (categorical variables)

Variable	*Category*	N	%
Biochemical relapse			
	No	104	69.8
	Yes	45	30.2
PSA (ng/ml)			
	<10	110	73.8
	>10	39	26.2
Margin status			
	Negative	89	59.7
	Positive	60	40.3
Nodes			
	Positive	1	0.7
Extracapsular			
	No	84	56.3
	Yes	65	43.6
Gleason score			
	$\leqslant 6$	74	49
	$=7$	64	42
	$\geqslant 8$	13	9

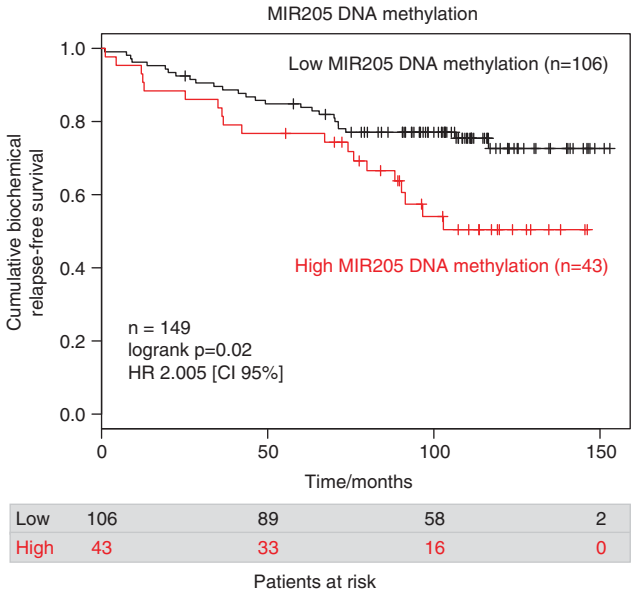

Figure 5. *MIR-205* DNA methylation is associated with prostate cancer outcome. Kaplan–Meier curves showing biochemical recurrence-free survival in prostate cancer patients. Patients stratified by *MIR-205* DNA methylation status (categorized as high and low based on the upper quartile of the median methylation values).

leukemia.[47] We report here, for the first time of an association between miRNA DNA hypermethylation and outcome in prostate cancer.

One limitation of this study is the relatively small number of clinical events such as development of metastases or death from prostate cancer. Hence, the association between *MIR-205* DNA methylation and prostate cancer progression should be tested and validated in locally advanced prostate cancer with longer follow-up time. In summary, the results presented here show a relationship between epigenetic repression of miR-205, elevation of MED1 levels, and suggest that *MIR-205* DNA methylation in prostate cancer may have potential as a prognostic biomarker.

MATERIALS AND METHODS

Cell lines and culture

LNCaP cells were propagated in T-media (Dulbecco's modified Eagle's medium low glucose supplemented with Kaign's F-12 medium, insulin, T3, transferrin, biotin, adenine, pen/strep, glutamine and 10% fetal calf serum), as described by Song *et al.*[48] PrEC cells were propagated in PrEGM (Lonza, Basel, Switzerland). PC3, DU145, MCF7 and MB231 cells were propagated in Dulbecco's modified Eagle's medium (Invitrogen) supplemented with 10% fetal calf serum. HMEC184 and 219 cells were propagated in MEGM media (Lonza). Cell lines were authenticated by short tandem repeat polymorphism, single-nucleotide polymorphism, and fingerprint analyses and passaged for <6 months. 5-Aza-2′-deoxycytidine (5-Aza-CdR) (Fluka) treatment was performed for 72 h with fresh media and drug added at 24 and 48 h. LNCaP were treated with 3 μM 5-Aza-CdR, and PrEC 1 μM 5-Aza-CdR following optimization based on reactivation of the imprinted gene *IGF2* and the prostate cancer hypermethylated gene *GSTP1* in response to treatment (data not shown).

RT–PCR analysis

Total RNA was isolated using Trizol reagent (Invitrogen). First-strand complementary DNA was synthesized using 1 μg RNA and superscript reverse transcriptase (Invitrogen). Complementary DNA was then subjected to 40 cycles of amplification, using temperature and Mg^{2+} optimized conditions, using either ABI7900 (Applied Biosystems, Foster City, CA, USA) or LightCycler480 (Roche, Basel, Switzerland) thermal cyclers. PCR products were verified by high resolution-melt and gel-electrophoresis. A table of primer sequences is listed in Supplementary Table S2. TaqMan assays for miR-205, β-actin, 18S and *RNU48* were obtained from Applied Biosystems. The *LOC642587* sequencing library was constructed using purified PCR product (PCR Pure Kit, Qiagen, Hilden, Germany), cloned into pGEM-T Easy Vector, before sequencing (Big Dye, Applied Biosystems).

DNA methylation assays

Genomic DNA was extracted using the Mammalian Blood and Tissue Kit (Qiagen). Sequenom MassArray DNA methylation analysis was performed as described previously.[49] Briefly, 1 μg of DNA was treated with sodium metabisulphite[50] and PCR amplified, thereby incorporating the T7 promoter sequence. Alkaline phosphatase treatment followed by *in vitro* transcription and cleavage by RNase A to result in specific fragmentation. The obtained mixture of fragments was subjected to matrix-assisted laser desorption/ionization time-of-flight mass-spectrometry (MALDI-TOF MS). Fragments containing one or more CpG sites were referred to as 'CpG units'. *SssI* (New England Biolabs, Ipswich, MA, USA) enzymatically methylated DNA, whole-genome amplified unmethylated DNA and a 50% methylated/unmethylated mix were included as controls. Two separate *MIR-205* MassArray assays were designed and used in this study; respective CpG sites and units are depicted in Supplementary Figure S2. Spike-in fully methylated DNA controls were detectable to 5 ng using the *MIR-205* MassArray clinical assay (data not shown).

H3K9 chromatin immunoprecipitation

LNCaP and PrEC cells fixed in 1% formaldehyde for 10 min before sodium dodecyl sulfate lysis and sonication. Immunoprecipitation was performed overnight at 4 °C with 10 μl anti-acetyl H3K9 (#06.599, Millipore, Billerica, MA, USA). DNA was eluted with 0.1M $NaHCO_3$, 1% sodium dodecyl sulfate elution buffer and reverse cross-linked. Immunoprecipitations and input controls were purified by phenol chloroform extraction and ethanol precipitation, as described previously.[51]

Transfection and cell growth assays

Cells were reverse transfected with synthetic pre-miR (Applied Biosystems) or LNA antisense oligonucleotides (Exiqon) to a final concentration of 50 nM using siPORT *NeoFX* transfection agent (Applied Biosystems). Twenty-four hours post transfection, the media was changed to T-media supplemented with 10% charcoal-stripped fetal calf serum. Transfectant concentrations were optimized with Cy3 labeled pre-miRs (Applied Biosystems), revealing $\sim>90\%$ transfection efficiency in both cell lines at the optimized concentration, as visualized by fluorescence microscopy. Efficacy of pre-miR transfection was first assessed in LNCaP cells by monitoring the capacity of pre-miR-1 to downregulate a known target gene, twinfilin-1 (*PTK9*);[52] this showed a 10-fold knockdown under our optimized conditions (data not shown). For cell viability assays, cells were seeded and reverse transfected as above at a density of 1×10^4 cells per well in 96-well microtiter plate. At 12 h fresh T-media supplemented with 10% charcoal-stripped fetal calf serum and dihydrotestosterone (DHT, Sigma-Aldrich, St Louis, MO, USA) was added to 10 nM final concentration or an equivalent volume of ethanol, as indicated. The CellTiter 96 Aqueous Non-Radioactive Cell Proliferation Assay (MTS; Promega, Madison, WI, USA) was performed as per the manufacturers' recommendations. Efficacy of miR-205 modulation was determined by TaqMan qPCR (Applied Biosystems), and is increased following pre-miR transfection (Supplementary Figure S4).

Antibodies and western blotting

Protein was extracted using radioimmunoprecipitation assay (RIPA) buffer with protease inhibitors (0.1 mM vanadate, 10 μg/ml leupeptin, 1 mM PMSF, 10 μg/ml aproptinin, 20 mM NaF). Twelve micrograms of lysates were separated by NuPAGE 3–8% Tris-Acetate gels (Invitrogen), and proteins were transferred to a nitrocellulose membrane (Amersham, Amersham, UK). Transfer efficiency was visualized using Ponceau S (Sigma-Aldrich). Membranes were blocked with 5% skim milk $1\times$ PBST, pH 7.4, before incubation with the following primary antibodies: MED1 total protein (AB64965; Abcam, Cambridge, MA, USA) MED1 phospho- (T1457) protein (AB60950; Abcam) and β-actin (A-5441, Sigma-Aldrich), overnight at 4 °C in blocking buffer. Secondary horse radish peroxidase conjugated antibodies were incubated for 1 h at room temperature. Proteins were visualized by chemiluminesence (PerkinElmer, Waltham, MA, USA), and densitometry

performed using Photoshop software (Adobe Systems, Mountain View, CA, USA).

Tumor samples

Fresh frozen clinical tissue samples were obtained from St Vincent's Campus Prostate Cancer Group from men with localized prostate cancer treated by radical prostatectomy, with appropriate ethical approval from St Vincent's Campus Research Ethics Committee (Approval No: H00/088). Patients were selected on the availability of fresh frozen samples for which full clinicopathological features and outcome data were available. Surgery was performed by one of six specialist urologists. Patients were followed postoperatively by their surgeons on a monthly basis until satisfactory urinary continence was obtained and then at 3-month intervals until the end of the first year, at six-monthly intervals to 5 years and yearly thereafter. Biochemical relapse was defined by the following criteria: biochemical disease progression with a serum PSA concentration $\geqslant 0.2$ ng/ml increasing over a 3-month period or local recurrence on digital rectal examination confirmed by biopsy or by a subsequent rise in PSA. Clinical recurrence was not considered due to the limited number of events at the time of writing (death from prostate cancer $n=3$, bony metastasis $n=2$, local metastasis $n=1$). Two patient cohorts were used. The discovery cohort consisted of 14 prostate cancers with seven cases having matched adjacent normal prostate tissue. The validation cohort consisted of 149 patients who had a radical prostatectomy performed between 1996 and 2003 (cohort Tables 1 and 2). All samples were histologically examined using hematoxylin and eosin stained frozen sections and was macrodissected to ensure a minimum of 70% tumor content. In the first cohort RNA and DNA were extracted by Trizol reagent (Invitrogen), in the second cohort DNA was extracted using the Puregene isolation kit (Qiagen), as per the manufacturers' instructions.

Statistical analysis

Biochemical relapse free survival was measured from the date of radical prostatectomy to relapse or the date of last follow-up. One-way analysis of variance tests were conducted to assess association between methylation levels and clinicopathological variables. Multivariate Cox models were produced by assessing *MIR-205* methylation with other baseline covariates of clinical relevance, such as Gleason grade, pathological stage and preoperative PSA, which were modeled as dichotomous or continuous variables as appropriate.[53] QRT–PCR experiments were analyzed using the delta-Ct method.[54] All *P*-values corresponded to two-sided tests unless otherwise stated and $P<0.05$ was considered statistically significant. Statistical analyses were performed using Microsoft Excel and the R software environment (R Foundation for Statistical Computing, Vienna, Austria).

ABBREVIATIONS

miRNA, microRNA; ChIP, chromatin immunoprecipitation; 5-Aza-CdR, 5-Aza-2′-deoxycytidine; IP, immunoprecipitation; FCS, fetal calf serum; CSFCS, charcoal-stripped fetal calf Serum; DHT, dihydrotestosterone; PSA, prostate specific antigen; AR, androgen receptor; BRFS, biochemical relapse free survival.

CONFLICT OF INTEREST

The authors declare no conflict of interest.

ACKNOWLEDGEMENTS

We would like to thank Gillian Lehrbach, Ann-Maree Haynes, Ruth Pe Benito and Clarisse Puno for technical assistance. This work is supported by Cancer Institute NSW (CINSW), Cure Cancer Australia fellowships (TH), and National Health and Medical Research Council and CINSW project grants (SJC).

REFERENCES

1 Jones PA, Baylin SB. The epigenomics of cancer. *Cell* 2007; **128**: 683–692.
2 Cooper CS, Foster CS. Concepts of epigenetics in prostate cancer development. *Br J Cancer* 2009; **100**: 240–245.
3 Carthew RW, Sontheimer EJ. Origins and mechanisms of miRNAs and siRNAs. *Cell* 2009; **136**: 642–655.
4 Cho WC. OncomiRs: the discovery and progress of microRNAs in cancers. *Mol Cancer* 2007; **6**: 60.
5 Ozen M, Creighton CJ, Ozdemir M, Ittmann M. Widespread deregulation of microRNA expression in human prostate cancer. *Onco* 2008; **27**: 1788–1793.
6 Rosenfeld N, Aharonov R, Meiri E, Rosenwald S, Spector Y, Zepeniuk M *et al.* MicroRNAs accurately identify cancer tissue origin. *Nat Biotech* 2008; **26**: 462–469.
7 Hulf T, Sibbritt T, Wiklund ED, Bert S, Strbenac D, Statham AL *et al.* Discovery pipeline for epigenetically deregulated miRNAs in cancer: integration of primary miRNA transcription. *BMC Genomics* 2011; **12**: 54.
8 Wu H, Zhu S, Mo YY. Suppression of cell growth and invasion by miR-205 in breast cancer. *Cell Res* 2009; **19**: 439–448.
9 Iorio MV, Casalini P, Piovan C, Di Leva G, Merlo A, Triulzi T *et al.* microRNA-205 Regulates HER3 in human breast cancer. *Cancer Res* 2009; **69**: 2195–2200.
10 Sempere LF, Christensen M, Silahtaroglu A, Bak M, Heath CV, Schwartz G *et al.* Altered microrna expression confined to specific epithelial cell subpopulations in breast cancer. *Cancer Res* 2007; **67**: 11612–11620.
11 Gandellini P, Folini M, Longoni N, Pennati M, Binda M, Colecchia M *et al.* miR-205 Exerts tumor-suppressive functions in human prostate through down-regulation of protein kinase Cepsilon. *Cancer Res* 2009; **69**: 2287–2295.
12 Neely LA, Rieger-Christ KM, Neto BS, Eroshkin A, Garver J, Patel S *et al.* A microRNA expression ratio defining the invasive phenotype in bladder tumors. *Urol Oncol* 2010; **28**: 39–48.
13 Childs G, Fazzari M, Kung G, Kawachi N, Brandwein-Gensler M, McLemore M *et al.* Low-level expression of microRNAs let-7d and miR-205 are prognostic markers of head and neck squamous cell carcinoma. *Am J Pathol* 2009; **174**: 736–745.
14 Feber A, Xi L, Luketich JD, Pennathur A, Landreneau RJ, Wu M *et al.* MicroRNA expression profiles of esophageal cancer. *J Thoracic Cardiovasc Surg* 2008; **135**: 255–260; discussion 60.
15 Chung TK, Cheung TH, Huen NY, Wong KW, Lo KW, Yim SF *et al.* Dysregulated microRNAs and their predicted targets associated with endometrioid endometrial adenocarcinoma in Hong Kong women. *Int J Cancer* 2009; **124**: 1358–1365.
16 Iorio MV, Visone R, Di Leva G, Donati V, Petrocca F, Casalini P *et al.* MicroRNA signatures in human ovarian cancer. *Cancer Res* 2007; **67**: 8699–8707.
17 Lebanony D, Benjamin H, Gilad S, Ezagouri M, Dov A, Ashkenazi K *et al.* Diagnostic assay based on hsa-miR-205 expression distinguishes squamous from nonsquamous non-small-cell lung carcinoma. *J Clin Oncol* 2009; **27**: 2030–2037.
18 Yanaihara N, Caplen N, Bowman E, Seike M, Kumamoto K, Yi M *et al.* Unique microRNA molecular profiles in lung cancer diagnosis and prognosis. *Cancer cell* 2006; **9**: 189–198.
19 Markou A, Tsaroucha EG, Kaklamanis L, Fotinou M, Georgoulias V, Lianidou ES. Prognostic value of mature microRNA-21 and microRNA-205 overexpression in non-small cell lung cancer by quantitative real-time RT-PCR. *Clin Chem* 2008; **54**: 1696–1704.
20 Fletcher AM, Heaford AC, Trask DK. Detection of metastatic head and neck squamous cell carcinoma using the relative expression of tissue-specific mir-205. *Trans Oncol* 2008; **1**: 202–208.
21 Yu J, Ryan DG, Getsios S, Oliveira-Fernandes M, Fatima A, Lavker RM. MicroRNA-184 antagonizes microRNA-205 to maintain SHIP2 levels in epithelia. *Proc Natl Acad Sci USA* 2008; **105**: 19300–19305.
22 Tran N, McLean T, Zhang X, Zhao CJ, Thomson JM, O'Brien C *et al.* MicroRNA expression profiles in head and neck cancer cell lines. *Biochem Biophys Res Comm* 2007; **358**: 12–17.
23 Gottardo F, Liu CG, Ferracin M, Calin GA, Fassan M, Bassi P *et al.* Micro-RNA profiling in kidney and bladder cancers. *Urol Oncol* 2007; **25**: 387–392.
24 Ryan DG, Oliveira-Fernandes M, Lavker RM. MicroRNAs of the mammalian eye display distinct and overlapping tissue specificity. *Mol Vis* 2006; **12**: 1175–1184.
25 Dijckmeester WA, Wijnhoven BP, Watson DI, Leong MP, Michael MZ, Mayne GC *et al.* MicroRNA-143 and −205 expression in neosquamous esophageal epithelium following Argon plasma ablation of Barrett's esophagus. *J Gastrointest Surg* 2009; **13**: 846–853.
26 Gregory PA, Bert AG, Paterson EL, Barry SC, Tsykin A, Farshid G *et al.* The miR-200 family and miR-205 regulate epithelial to mesenchymal transition by targeting ZEB1 and SIP1. *Nat Cell Biol* 2008; **10**: 593–601.
27 Chi SW, Zang JB, Mele A, Darnell RB. Argonaute HITS-CLIP decodes microRNA-mRNA interaction maps. *Nature* 2009; **460**: 479–486.
28 Baek D, Villen J, Shin C, Camargo FD, Gygi SP, Bartel DP. The impact of microRNAs on protein output. *Nature* 2008; **455**: 64–71.
29 Majid S, Dar AA, Saini S, Yamamura S, Hirata H, Tanaka Y *et al.* MicroRNA-205-directed transcriptional activation of tumor suppressor genes in prostate cancer. *Cancer* 2010; **116**: 5637–5649.
30 Mouillet JF, Chu T, Nelson DM, Mishima T, Sadovsky Y. MiR-205 silences MED1 in hypoxic primary human trophoblasts. *FASEB J* 2010; **24**: 2030–2039.

31 Wang Q, Sharma D, Ren Y, Fondell JD. A coregulatory role for the TRAP-mediator complex in androgen receptor-mediated gene expression. *J Biol Chem* 2002; **277**: 42852–42858.
32 Wang Q, Carroll JS, Brown M. Spatial and temporal recruitment of androgen receptor and its coactivators involves chromosomal looping and polymerase tracking. *Mol Cell* 2005; **19**: 631–642.
33 Kouzarides T. Chromatin modifications and their function. *Cell* 2007; **128**: 693–705.
34 Damber JE, Aus G. Prostate cancer. *Lancet* 2008; **371**: 1710–1721.
35 Vijayvargia R, May MS, Fondell JD. A coregulatory role for the mediator complex in prostate cancer cell proliferation and gene expression. *Cancer Res* 2007; **67**: 4034–4041.
36 Belakavadi M, Pandey PK, Vijayvargia R, Fondell JD. MED1 phosphorylation promotes its association with mediator: implications for nuclear receptor signaling. *Mol Cell Biol* 2008; **28**: 3932–3942.
37 Wiklund ED, Bramsen JB, Hulf T, Dyrskjot L, Ramanathan R, Hansen TB *et al.* Coordinated epigenetic repression of the miR-200 family and miR-205 in invasive bladder cancer. *Int J Cancer* 2010; **128**: 1327–1334.
38 Ke XS, Qu Y, Rostad K, Li WC, Lin B, Halvorsen OJ *et al.* Genome-wide profiling of histone h3 lysine 4 and lysine 27 trimethylation reveals an epigenetic signature in prostate carcinogenesis. *PLoS ONE* 2009; **4**: e4687.
39 Karginov FV, Cheloufi S, Chong MM, Stark A, Smith AD, Hannon GJ. Diverse endonucleolytic cleavage sites in the mammalian transcriptome depend upon microRNAs, Drosha, and additional nucleases. *Mol Cell* 2010; **38**: 781–788.
40 Koschubs T, Lorenzen K, Baumli S, Sandstrom S, Heck AJ, Cramer P. Preparation and topology of the Mediator middle module. *Nucleic Acids Res* 2010; **38**: 3186–3195.
41 Zhu Y, Qi C, Jain S, Le Beau MM, Espinosa 3rd R, Atkins GB *et al.* Amplification and overexpression of peroxisome proliferator-activated receptor binding protein (PBP/PPARBP) gene in breast cancer. *Proc Natl Acad Sci USA* 1999; **96**: 10848–10853.
42 Jia L, Coetzee GA. Androgen receptor-dependent PSA expression in androgen-independent prostate cancer cells does not involve androgen receptor occupancy of the PSA locus. *Cancer Res* 2005; **65**: 8003–8008.
43 Paoletti AC, Parmely TJ, Tomomori-Sato C, Sato S, Zhu D, Conaway RC *et al.* Quantitative proteomic analysis of distinct mammalian Mediator complexes using normalized spectral abundance factors. *Proc Natl Acad Sci USA* 2006; **103**: 18928–18933.
44 Kornberg RD. Mediator and the mechanism of transcriptional activation. *Trends in Biochemsci* 2005; **30**: 235–239.
45 Platica M, Verma RS, Macera MJ, Platica O. LNCaP-OM, a new androgen-resistant prostate cancer subline. *In Vitro Cell Dev Biol Anim* 1997; **33**: 147–149.
46 Devaney J, Stirzaker C, Qu W, Song JZ, Statham AL, Patterson KI *et al.* Epigenetic deregulation across 2q14.2 differentiates normal from prostate cancer and provides a regional panel of novel DNA methylation cancer biomarkers. *Cancer Epidemiol Biomarkers Prev* 2011; **20**: 148–159.
47 Agirre X, Vilas-Zornoza A, Jimenez-Velasco A, Martin-Subero JI, Cordeu L, Garate L *et al.* Epigenetic silencing of the tumor suppressor microRNA Hsa-miR-124a regulates CDK6 expression and confers a poor prognosis in acute lymphoblastic leukemia. *Cancer Res* 2009; **69**: 4443–4453.
48 Song JZ, Stirzaker C, Harrison J, Melki JR, Clark SJ. Hypermethylation trigger of the glutathione-S-transferase gene (GSTP1) in prostate cancer cells. *Oncogene* 2002; **21**: 1048–1061.
49 Coolen MW, Statham AL, Gardiner-Garden M, Clark SJ. Genomic profiling of CpG methylation and allelic specificity using quantitative high-throughput mass spectrometry: critical evaluation and improvements. *Nucleic Acids Res* 2007; **35**: e119.
50 Clark SJ, Harrison J, Paul CL, Frommer M. High sensitivity mapping of methylated cytosines. *Nucleic Acids Res* 1994; **22**: 2990–2997.
51 Coolen MW, Stirzaker C, Song JZ, Statham AL, Kassir Z, Moreno CS *et al.* Consolidation of the cancer genome into domains of repressive chromatin by long-range epigenetic silencing (LRES) reduces transcriptional plasticity. *Nat Cell Biol* 2010; **12**: 235–246.
52 Lim LP, Lau NC, Garrett-Engele P, Grimson A, Schelter JM, Castle J *et al.* Microarray analysis shows that some microRNAs downregulate large numbers of target mRNAs. *Nature* 2005; **433**: 769–773.
53 Horvath LG, Henshall SM, Kench JG, Saunders DN, Lee CS, Golovsky D *et al.* Membranous expression of secreted frizzled-related protein 4 predicts for good prognosis in localized prostate cancer and inhibits PC3 cellular proliferation in vitro. *Clin Cancer Res* 2004; **10**: 615–625.
54 Livak KJ, Schmittgen TD. Analysis of relative gene expression data using real-time quantitative PCR and the 2(-Delta Delta C(T)) method. *Methods* 2001; **25**: 402–408.

Supplementary Information accompanies the paper on the Oncogene website (http://www.nature.com/onc)